

Research Journal of Pharmaceutical, Biological and Chemical Sciences

Preparation Characterization of In-Situ Prepared Silver/PVDF-PVP Nano-Composites

AM Abdelghany^a, EM Abdelrazek^b, AH Oraby^b, and E Lasheen^b

^a Spectroscopy Department, Physics Division, National Research Center, Dokki, 12311, Egypt

^b Physics Department, Faculty of Science, Mansoura University, Mansoura 35516, Egypt,

ABSTRACT

Ag nanoparticles supported (Ag NPs) within Polyvinylidene fluoride (PVDF)/polyvinyl pyrrolidone (PVP) films have been successfully synthesized using novel in situ method. PVDF and PVP acted as a stabilizer and polyol reductant, respectively. The successful incorporation of silver nanoparticles in PVDF/PVP matrix was confirmed by UV-Vis spectroscopy, X-ray diffraction (XRD), transmission electron microscope (TEM), Fourier transform infrared (FTIR) spectroscopy and Differential scanning calorimeter (DSC). It was found that PVDF/PVP-stabilized silver nanocomposite film revealed the presence of well-dispersed and spherical silver nanoparticles with an average diameter of 9 nm, while the particle sizes were increased as the AgNO₃ percentage increased. A possible formation mechanism of Ag nanoparticles is also proposed in this article.

Keywords : PVDF; PVP; AgNO₃; FTIR; UV-Vis.; TEM.

**Corresponding author*

INTRODUCTION

The preparation and study of nano-size material is an interesting topic in research and technology because of increasing their applications in electronic industry [1] and medical science [2-4] due to increasing of their unique character differing from the bulk state of those [5]. Phenomena at the nanoscale are likely to be a completely new world, where properties may not be predictable from those observed at large size scales, on account of quantum size effect and surface effects. Although many approaches to obtain nanocomposites involve the *in situ* reduction of metal salts, [6-7] they lack control on monodispersity, particle size and shape and even composition, resulting in a poor control of their properties. Therefore, methods based on the doping of polymers or glasses with preformed nanoparticles are becoming more and more popular in the last years since they allow engineering nano-composites with well-defined properties [8–10]. Nevertheless, it is not straightforward to transfer the nanoparticles into solid substrates with high optical quality while retaining the characteristic properties of single particles, i.e., preventing aggregation.

Due to the specific size, shape, and distribution, nanoparticles are used in the production of novel systems such as nanosensors [11], nanoresonators [12], nanoactuators [13], nanoreactors [14], single electron tunneling devices [15], plasmonics [16], and nanowire based devices [17] etc. This fact often requires the nanoparticles surface modification with an appropriate molecule or coating to maintain the colloidal stability during the process [8–10]. Silver has been one of the main materials investigated due to its chemical stability, good thermal and electrical conductivity and catalytic properties. Studies of silver nanoparticles (Ag NPs) in different polymers have been reported, for example, the synthesis in polyvinylpyrrolidone (PVP), [18] polyvinyl alcohol (PVA), [19] hyper branched polyurethane (HP) [20] and polyacrylonitrile (PAN) [21] among others [22] to yield discrete silver nanoparticles. Significant variations can be obtained on the average sizes and shapes of the silver nanoparticles, depending on the specific polymers used, due to the different chemical structures and silver–polymer interactions.

Polyvinylidene fluoride (PVDF) has strongly attracted the attention of researchers because of its high piezoelectricity, chemical resistance, mechanical strength and process ability [23]. Recently, PVDF has been widely used in biotechnology [24], biomedical sectors [25], photo recording [26] and microwave modulation [27].

PVDF is known as to be semi-crystalline polymer which may contain one or more crystalline form: α , β , γ and δ [28]. The β -phase contains trans-planar (TT) chains, while the α -phase has a random combination of trans-gauche isomers (TG^+ , TG^- , $T3G^+$ and $T3G^-$). The β form is the most interesting one because it is polar, and it is responsible for piezoelectricity. However, α form, which is non-polar, also has a considerable piezoelectric effect [29].

Chae et al. [30] studied the influence of high contents of Ag NPs on the properties of β -PVDF. As a result of the doping, increases of the thermal stability and the degree of crystallinity of the composite have been observed. Regarding other silver Nano composites, Bozanic et al.

[31] doped a biopolymeric matrix (sago starch) with Ag and Ag₂S, detecting the presence of surface Plasmon resonance (SPR) bands for the higher nanoparticle concentrations. The uniform distribution of the Ag NPs was studied by Compton et al. [32].

In the present work, Ag NPs doped with PVP and were blended with PVDF for different Ag NPs concentrations. The influence of the dispersed Ag NPs on the degree of crystallinity of the composites was investigated. The SPR-related optical response of the nanoparticles was studied by UV-visible spectroscopy.

EXPERIMENTAL DETAILS

Silver nitrate (AgNO₃, 98%) was purchased from Aldrich. Dimethylformamide (DMF, pure grade), Poly (vinilidene fluoride) (PVDF Alfa Aesar, A Johnson matthey company, CAS: 24937-79-9), Polyvinylpyrrolidone (Sisco research laboratories pvt.ltd, Mumbai-400, India, Mw 40000). Equal mass fractions of PVDF and PVP (50/50 wt %) was dissolved in pure DMF separately, AgNO₃ was added to dissolved PVP and left until pale yellow color appears and then added to the dissolved PVDF. Polymer blend solution was stirred continuously until a homogeneous viscous liquid was formed. The resulting solution was left 48 hours at 323 K. The mixture was cast on to a glass dish and kept at 323 °K for 2 days to remove the solvent traces.

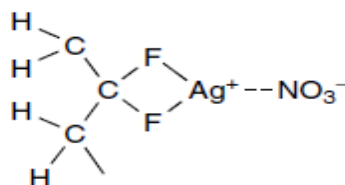
Film thickness in the range of 0.07–0.10 mm was obtained. AgNO₃ of different mass fractions ($x = 0.0, 0.01, 0.05, 0.1, 0.2$ and 0.4 %) were prepared. X-ray diffraction scans (XRD) were obtained using PANalytical X`Pert PRO XRD system using CuK_α radiation (where, $\lambda = 1.540$ Å, the tube operated at 30 kV, the Bragg's angle (2θ) in the range of 5-80°). FT-IR absorption spectra were carried out using the single beam Fourier transform-infrared spectrometer (Nicolet iS10, USA). FT-IR spectra of the samples were obtained in the spectral range of 4000–400 cm⁻¹. UV/Vis. absorption spectra were measured in the wavelength region of 265-900 nm using a spectrophotometer (JASCO V-500/V-600 series Spectrophotometer, Japan). Transmission Electron Microscopy (TEM) (JEOL JEM 1010 transmission electron microscope operating at an acceleration voltage of 100 kV). A set of five homogeneous samples named: S0 (pure blend (PVDF/PVP)), S1 (0.01 M of AgNO₃), S2 (0.05 M of AgNO₃), S3 (0.1 M of AgNO₃), S4 (0.2M of AgNO₃) and S5 (0.4M of AgNO₃).

RESULTS AND DISCUSSION

X-ray diffraction (XRD)

X-ray diffraction patterns of all samples are shown in figure (1). The spectra of PVDF indicate the presence of semi-crystalline structures. There are two intense peaks appearing at diffraction angles $2\theta = 20.02^\circ$ and 39.15° , assigning to β and α -PVDF phases, respectively. The peak at $2\theta = 20.02^\circ$ (110 or 200) for β -phase and at 39.15° (002) for α -phase for pure PVDF [33]. Two typical peaks at $2\theta = 10.9^\circ$ and 21.4° were observed for PVP [34]. Upon blending with PVP and AgNO₃ addition to PVDF matrix, there was a noticeable change in the intensity of XRD peaks of the doped samples as well as the appearance of additional peaks. In addition to the

main intensity peak at $2\theta = 20.5^\circ$ decrease with increasing AgNO_3 until S3. It is clear that the degree of crystallinity of β -phase is decreased by the AgNO_3 filler. In the case of S4 and S5, the main intensity peak at $2\theta = 20.5^\circ$ began to increase. The increase of the degree of crystallinity, for S4 and S5, can be explained by assuming that the excess AgNO_3 molecules may attach to the PVDF chain via fluorine bridges, as shown below:



The presence of peaks at 2θ values 39° and 43.4° corresponds to (111) and (200) planes of silver, respectively. Thus, the XRD spectrum confirmed the crystalline structure of silver nanoparticles. All the peaks in the XRD pattern can be readily indexed to a face-centered cubic structure of silver [35].

The average crystalline size of Ag nanoparticle was estimated for S5 at 2θ values 39° and 43.4° using Debye–Scherrer diffraction formula [25]:

$$D = \frac{k \lambda}{\beta \cos \theta} \tag{1}$$

Where $k = 0.9$, $\lambda = 1.541 \text{ nm}$ and β is the half-width of the diffraction peak. The calculated values of the crystallite size were 5.2 and 4.97nm for samples S5 at 2θ values 39° and 43.4° , respectively.

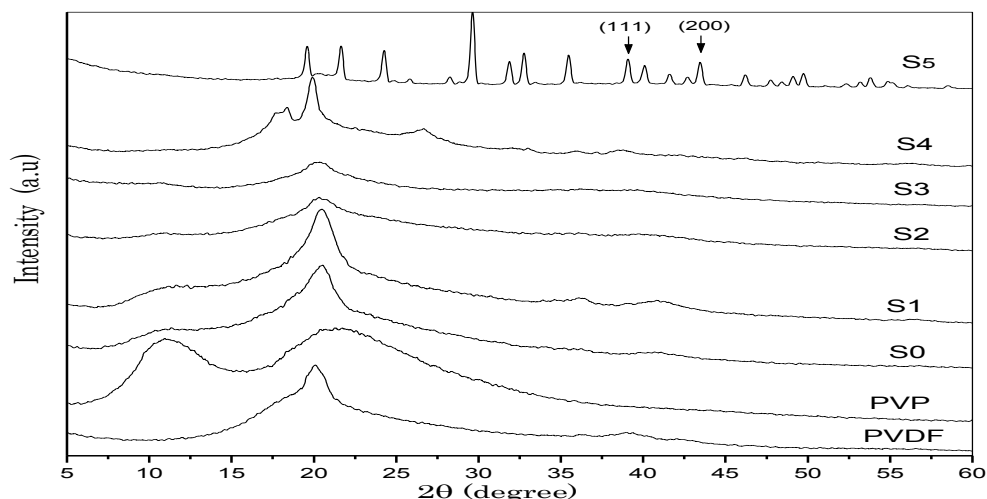


Fig.1: X-ray diffraction patterns of pure PVDF, PVP, Pure blend PVDF/PVP and different PVDF/PVP films filled with AgNO_3

Fourier Transform Infrared Studies

Figure (3) shows the FT-IR spectra of virgin PVDF, PVP, pure blend (PVDF/PVP) and its various concentrations of AgNO_3 with a pure blend in the spectral range $4000\text{-}400\text{ cm}^{-1}$.

In these spectra, the α -phase is evidenced particularly by the peaks $435, 486, 603$ and 768 cm^{-1} , while the β -phase is characterized by the peaks at 510 and 838 cm^{-1} [36]. Structures of PVDF are summarized in Table (1). The peaks at 510 cm^{-1} , belonging to the β -phase, are assigned to CF_2 bending and wagging modes [37]. The band at 836 cm^{-1} is assigned to CH_2 bending deformation, belonging to the β -phase [38].

For pure PVP, the absorption bands at 1660 cm^{-1} is assigned to the characteristic vibration of $\text{C}=\text{O}$ stretching, which is suitable site for polarons in (PVDF/PVP) matrices [39]. The vibrational band observed at 1289 cm^{-1} may be attributed to $\text{C}-\text{N}$ stretching of PVP [40].

With respect to the nature of the interaction between PVDF/PVP, it's assumed that the quasi hydrogen-bonding occurs due to the fact that the hydrogen atoms of PVDF possess acidity and the oxygen atoms of PVP offer electronegativity. A comparison of FT-IR spectra of pristine PVDF, PVP with the pure blend clearly shows the occurrence of the hydrogen bonding figure (3). The intensity of the carbonyl absorption band of PVP located at 1662 cm^{-1} increase when PVP blended with PVDF. This observation can be interpreted the effect of forming hydrogen bond between the carbonyl group and the methylene group, figure (2) The hydrogen bonding restricts the vibration of $\text{C}=\text{O}$ bond and hence increases the absorption intensity [41]. A new absorption peak placed at 974 cm^{-1} was appeared in the vibrational spectrum with addition of AgNO_3 . This peak can be characterized to α -phase of PVDF.

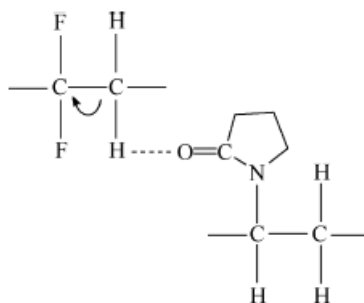


Fig.2: hydrogen bond between PVDF and PVP

Table 1: Structural assignments of vibrational frequencies for PVDF.

Band	Phase	Group and vibrational modes	Assignment
510	β	CF_2 bending	[37]
836	β	CH_2 rocking	[38]
883	β	CF_2 symmetric stretching	[42]
1072	β	CH_2 wagging	[37]
1238	β	CF out-of-plane deformation	[37]

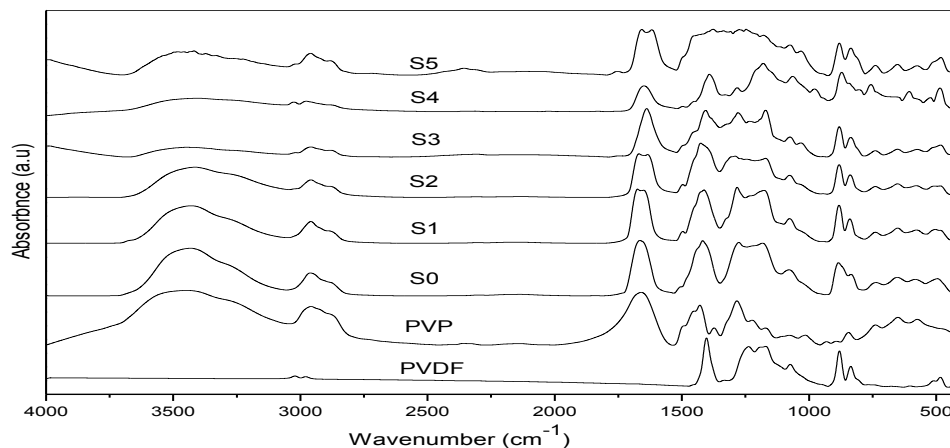


Fig.3: FT-IR of pure PVDF, PVP, Pure blend PVDF/PVP and different PVDF/PVP films filled with AgNO_3

UV/Vis. optical absorption

Figure (4) displays the UV–Vis absorption spectra of the prepared films. UV–Vis. absorption spectrum of pure blend PVDF/PVP shows an absorption band at 270 nm may be assigned to $\pi \rightarrow \pi^*$. This transition was related to the carbonyl groups ($\text{C}=\text{O}$) of PVP. UV–Vis. spectrum of PVDF/PVP/Ag film shows absorption peak at 414 nm. The absorbance band at 414 nm is attributed to the surface plasmon resonance phenomenon of free electrons in the conduction bands of Ag nanoparticles. This result is in complete agreement for those Ag nanoparticles were prepared [35]. The spontaneous formation of Ag NPs can be attributed to the direct redox between PVP and Ag^+ . The peak is shifted to higher wavelengths as AgNO_3 contents increase. The intensity of these bands was increased as the AgNO_3 contents increased in the system indicates that the concentration of Ag NPs increases. Hence, the absorption edge can be used to determine the blue shifted the optical energy of the nanoparticles using the relation:

$$E_g = \frac{hc}{\lambda} \quad (1)$$

where h is the Planck's constant and C is speed of light. According to Mott and Davis formula [44] the values of direct and indirect energy band gap (E_g) were obtained from the spectra by extrapolating the straight line plot of $(\alpha hv)^2$ versus (hv) and $(\alpha hv)^{1/2}$ versus (hv) , respectively (Fig.5a, b describe an example for calculating energy gap for pristine blend). Where α is the absorption coefficient which determined using the following relation [45]:

$$\alpha = \frac{2.303 A}{d} \quad (2)$$

where A is the absorbance and d is the thickness of the sample.

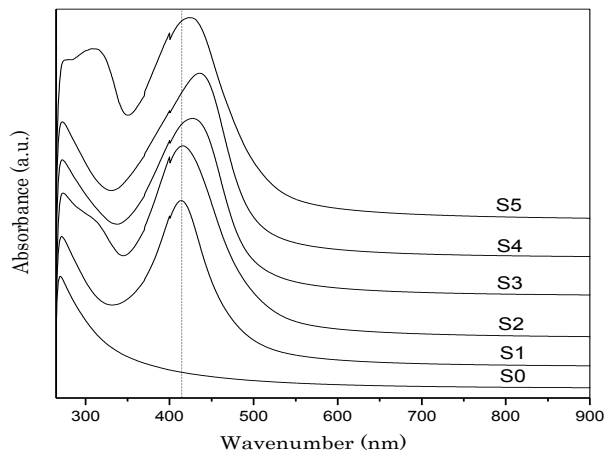
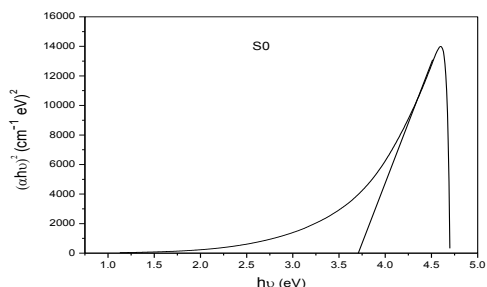


Fig. 4: UV-Vis. spectra for PVDF/PVP blend and with different concentrations of AgNO₃

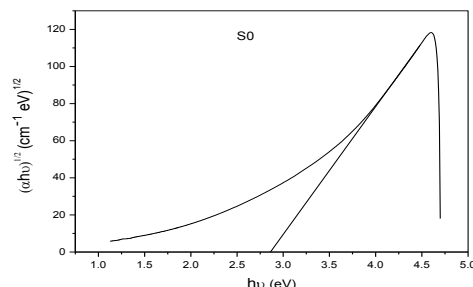
Table (2) shows the values of sharp edge, direct and indirect energy band gap. It is observed in the table that the band gap decrease with a variation of AgNO₃ with a fixed amount of the blend is attributed to the strong quantum confinement effect of Ag NPs. It is observed that PVDF/PVP blend-capped Ag NPs were more stable (did not suffer any observable changes after 1 week) than Ag NPs without polymer where, pure Ag NPs were precipitated after reaction from the solution.

Table 2: The absorption edge, band gap energy estimated from UV-Vis. absorption spectra

Sample	Absorption edge λ_g (nm)	Direct band gap E_{dg} (eV)	Indirect band gap E_{ig} (eV)
S0	423	3.66	2.93
S1	452	3.52	2.74
S2	466	3.46	2.66
S3	504	3.27	2.46
S4	519	3.11	2.39
S5	444	3.25	2.79



(a)



(b)

Fig.5: Direct and indirect optical band gap calculations for pure blend.

Transmission electron microscopy (TEM)

Transmission electron microscopy (TEM) is considered as one of the most important conformational tool in this work. Figure (6) shows TEM images of the distribution and the morphology with the particle size histogram of Ag NPs dispersed within PVDF/PVP polymer blend.

Image (S1) demonstrated the nanoparticles films with 0.01 M of Ag. The single particles have size in the range of 4 nm, which was consistent with UV-Vis and X-ray results and when the amount of AgNO_3 was increased to 0.4 M (S5), the size of Ag nanoparticles were increased to the range from 15 nm. At the amount of Ag nanoparticles was increased to 0.4 M (S5), the aggregation of Ag nanoparticles appeared and have size become in the range from 4 to 15 nm.

As shown in these images higher density particles were clearly and tiny spherical shapes.

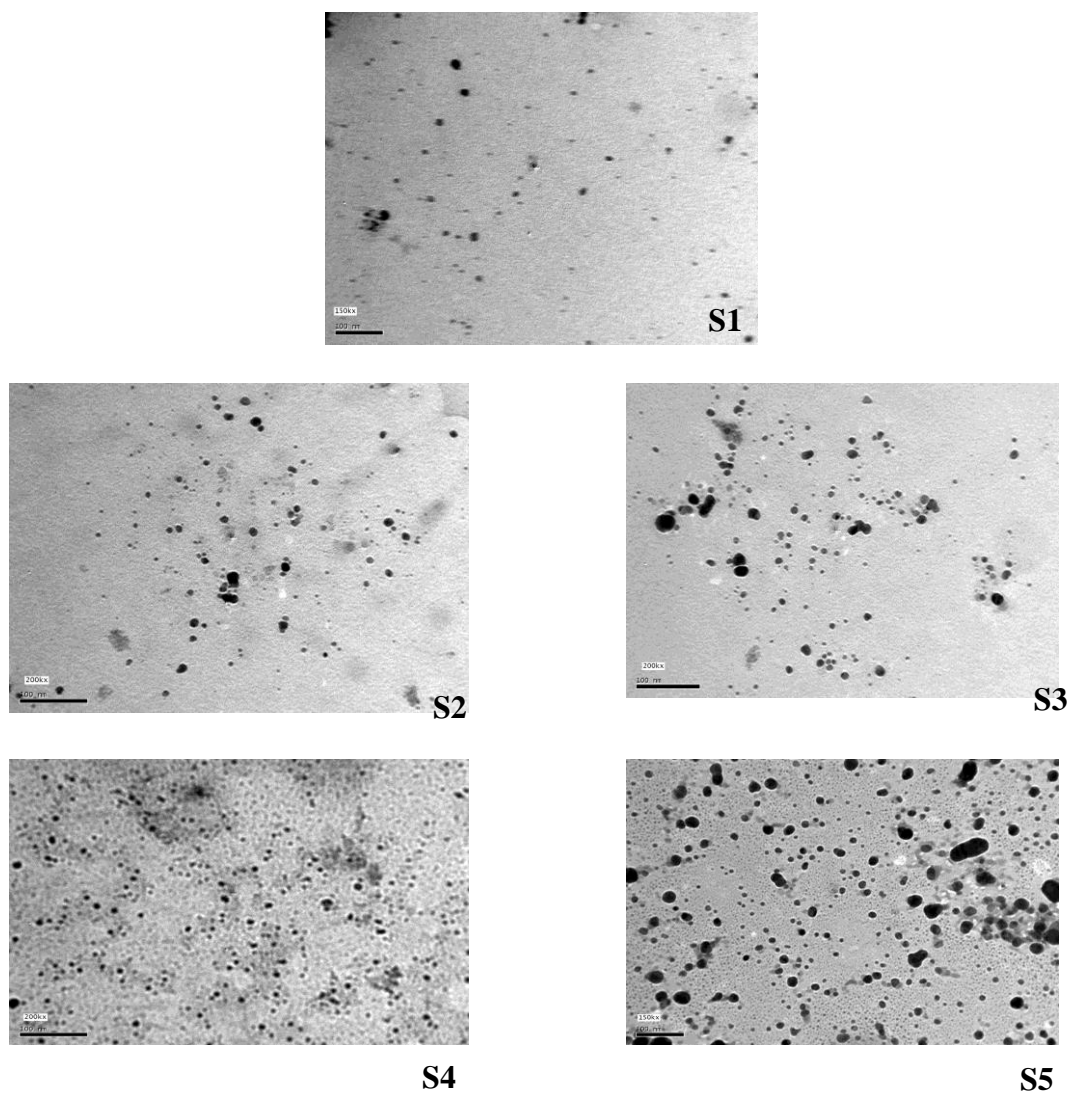


Fig.6: TEM images for PVDF/PVP blend and with different concentrations of AgNO_3

It is clear that from the histogram, the nanoparticles exhibit a uniform spherical shape and distribution with average size 9 nm. The average size was increased with the amount of Ag nanoparticles increases. From the UV–Vis spectra, X-ray diffraction and TEM images; it is found that a higher amount of Ag nanoparticles gave a larger size of Ag nanoparticles with a good dispersed within polymeric matrix. Based the above results and images, we observed that PVDF/PVP blend played an important role, effective surfactant and in controlling of the size and growth of Ag nanoparticles.

Electrical properties

DC electrical conductivity (σ) values can be calculated from the following equation:

$$\sigma = \frac{L}{R.A} \quad (3)$$

where L is the thickness in cm, R is the resistance in ohm and A is the surface area of the sample in cm^2 . the temperature dependent DC conductivity measurements were carried out in a temperature range of 373-453 K to analyze the mechanism of the conduction for the present system.

Figure (7) shows the variation of DC conductivity ($\ln \sigma$) with the reciprocal of the absolute temperature ($1000/T \text{ K}^{-1}$) for the polymer filled with different concentrations of AgNO_3 . It is clear that the conductivity values increase with increasing temperature for all samples. This can be explained with the help of free volume theory [46]. As the temperature increases, thermal movement of polymer chain segments and the dissociation of salts would be improved, this increased ionic conductivity for the prepared samples. As the temperature increases, the polymer can expand easily and produce free volume around polymer chains. Thus, ions, solvated molecules or polymer segments can move to the free volume. So, according to the free volume theory of polymers, when the temperature is increased the vibrational energy of a segment is sufficient to push against the hydrostatic pressure imposed by its neighbors and create a small amount of space surrounding its own volume in which vibrational motion can occur.

The resulting conductivity is represented by the overall mobility of ions and polymer, which is determined by the free volume around the polymer chain. Therefore, an increase in temperature produces more free volume, which increases the mobility of ions and segments that will assist ion transport and practically compensate the retarding effect of the ion clouds and hence the conductivity [47]. From the figure (7) clear that the electrical conductivity (σ) of the samples was changed within the range 1.79×10^{-8} to 7.5×10^{-7} S/m (at $T=453$ K), which suggests AgNO_3 as good filler to improve the electrical conductivity of the films.

We cannot measure the sample S5 due to aggregation of AgNO_3 on the sample's surface which became conducting sample at room temperature.

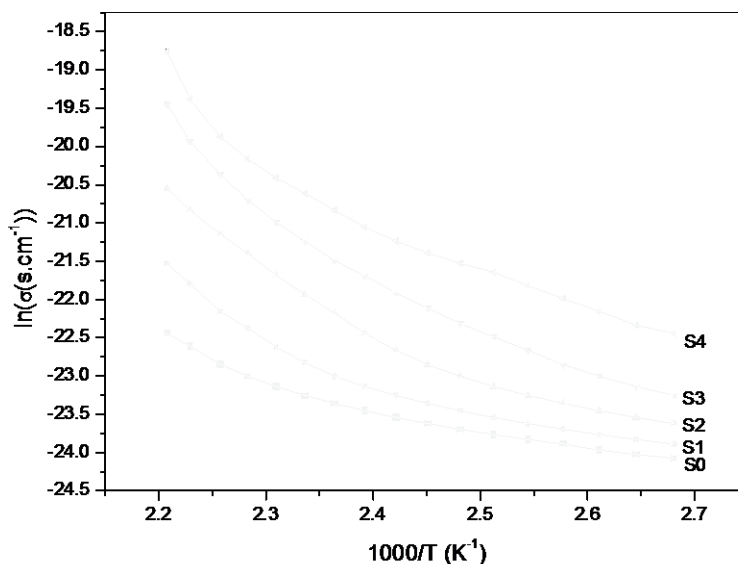


Fig.7: Variation of DC conductivity ($\ln \sigma$ ($S. cm^{-1}$)) with the reciprocal of absolute temperature ($1000/T$ (K^{-1})) for 0.0, 0.01, 0.05, 0.1 and 0.2% $AgNO_3$ filled PVDF/PVP sample

CONCLUSIONS

XRD spectrum confirmed the formation crystalline structure of silver nanoparticles. The average crystalline size of Ag nanoparticle in the range from 4 to 15 nm. FT-IR show that the interaction between PVDF/PVP occurs due to the fact that the hydrogen atoms of PVDF possess acidity and the oxygen atoms of PVP offer electronegativity. The excess $AgNO_3$ molecules may attach to the PVDF chain via fluorine bridges.

UV-Vis. absorption spectrum shows absorption peak at 414 nm is attributed to the surface Plasmon resonance phenomenon of free electrons in the conduction bands of Ag nanoparticles. It is observed that the band gap decrease with a variation of $AgNO_3$ with a fixed amount of the blend is attributed to the strong quantum confinement effect of Ag NPs. It is observed that PVDF/PVP blend-capped Ag NPs were more stable than Ag NPs without polymer where, pure Ag NPs were precipitated after reaction from the solution.

REFERENCES

- [1] M Hosokawa, K Nogi, M Naito, T Yokoyam. Nanoparticle Technology Handbook, Jordan Hill, Oxford UK 2008; 113- 176.
- [2] B Haley, E Frenkel. Urologic Oncology: Seminars and Original Investigation 2008; 26(1): 57.
- [3] JS Kim, E Kuk, KN Yu, J H Kim, SJ Park, H Kim. Nanomedicine: Nanotechnology, Biology and Medicine 2007; 3(1): 95.
- [4] M Rai, A Yadav, A Gade. Biotechnology Advances 2009; 27(1): 76.

- [5] T Liu, H Shao, J Phys. Condense Matter 2003; 15(17): 2507.
- [6] S Manna, SK Batabyal, AK Nandi. J Phys Chem B 2006; 110(25): 12318.
- [7] PW Wu, W Cheng, IB Martini, B Dunn, BJ Schwartz, EY Ablonovich. Adv Mater 2000; 12(19): 1438.
- [8] IP Astoriza-Santos, J Pérez-Juste, G Kick Elbick, LM Liz-Marzn. J Nanosci Nanotechnol 2006; 6 (1): 453.
- [9] VI Boe v, J Pérez-Juste, IP Astoriza-Santos, CJR Silv, MJM Gomes, LM Liz-Marzn. Langmuir 2004; 20(23): 10268.
- [10] J Pérez-Juste, MA Correa-Duarte, LM Liz-Marzn. Appl Surf Sci 2004; 226(1): 137.
- [11] OD Velev, EW Kaler. Langmuir 1999; 15(11): 3693.
- [12] KL Ekinci, XMH Huang, ML Roukes. Appl Phys Lett 2004; 84(22): 4469.
- [13] WC Lee, YH Cho. Curr Appl Phys 2007; 7(2): 139.
- [14] C Roos, M Schmidt, J Ebenhoch, F Baumann, B Deubzer, J Weis. Adv Mat 1999; 11(9): 761.
- [15] SH Hong, HK Kim, KH Cho, SW Hwang, JS Hwang, D Ahn. J Vac Sci Technol B 2006; 24(6): 136.
- [16] JR Krenn, JC Weeber, A Dereux, E Bourillot, JP Goudonnet, G Schider, AR Leitner. Phys Rev B 1999; 60(1): 5029.
- [17] Y Huang, X Duan, Q Wei, CM Lieber. Science 2001; 291: 630.
- [18] M Zheng, M Gu, Y Jin, G Jin. Mater Res Bull 2001; 36(4): 853.
- [19] PK Khanna, N Singh, S Charan, VVVS Subbarao, R Gokhale, UP Mulik. Mater Chem Phys 2005; 93(1): 117.
- [20] HW Lu, SH Liu, XL Wang, XF Qian, J Yin, ZK Zhu. Mater Chem Phys 2003; 81(1): 104.
- [21] Z Zhang, L Zhang, S Wang, W Chen, Y Lei. Polymer 2001; 42(19): 8315.
- [22] SH Lee, K Sung, TM Chung, SG Lee, KD Min, S Koo, CG Kim. J Nanosci Nanotechnol 2008; 8(9): 4734.
- [23] JM Brynaet, N Jongen, JL Dewez. J Polym Sci Polym Chem Ed 1997; 35: 1227.
- [24] SP Nunes, KV Peinemann, J Membr Sci 1992 ; 73(1): 25.
- [25] RF Valentini, TG Vargo, JAJr Gardella, P Aebischer. J Biomater Sci Polym Ed., 1993;5(1-2): 13.
- [26] A Tawansi, AH Oraby, E Ahmed, EM Abdelrazek, M Abdelaziz. J Appl Polym Sci 1998;70(9): 1759.
- [27] A Tawansi, MI Ayad, EM Abdelrazek. J Appl Polym Sci 1999;72(6): 771.
- [28] SP Bodhane, VS Shirodkar. J Appl Polym Sci 1999;74(6): 1347.
- [29] H Ohigashi. J Appl Phys 1976;47 (3): 949.
- [30] DW Chae, SS Hwang, SM Hong, SP Hong, BG Cho, BC Kim. Mol Cryst Liq Cryst 2007;464(1): 233.
- [31] DK Bozanic, V Djokovic, J Blanusa1, PS Nair , MK Georges, T Radhakrishnan. Eur Phys J E 2007;22(1): 51.
- [32] J Compton, D Kranbuehl, G Martin, E Espuche, L David. Macromol Symp 2007;247(1): 182.
- [33] GT Davis, JE McKinney, MG Broadhurst, SC Roth. J Appl Phys 1978; 49(10): 4998.
- [34] XG Li, I Kresse, J Springer, J Nissen, YL Yang. Polymer 2001;42(16): 6859.



- [35] M Sathishkumar, K Sneha, SW Won, CW Cho, S Kim, YS Yun. *Colloids Surfaces B* 2009;73(2): 332.
- [36] JrR Gregorio. *J Appl Polym Sci* 2006;100(4): 3272.
- [37] T Bocaccio, A Bottino, G Capanelli Piaggio. *J Membr Sci* 2000;210(2): 315.
- [38] A Salimi, AA Yousefi. *Polym Tes* 2003;22(6): 699.
- [39] N Chen, L Hong. *Polymer* 2002;43(4): 1429.
- [40] GNH Kumar, JL Rao, NO Gopal, KV Narasimulu, RPS Chakradhar, AV Rajulu. *Polymer* 2004;45(18): 5407.
- [41] IS Ellshmawi, AM Abdelghany, NA Hakeem. *Journal of materials science; Materials in Electronics* 2013;24(8): 2956.
- [42] N Chen, L Hong. *Polymer* 2002;43(4): 1429.
- [43] JL Li, CL Wang, WL Zhonghang, QH Webb, JF Webb. *Appl Phys Lett* 2002;81(12): 2223.
- [44] G Dong, X Xiao, X Liu, B Qian, Z Ma, S Chen, J Qiu. *J Nanopart Res* 2010;12(8): 1319.
- [45] AM Abdelghany, HA ElBatal, L Mari. *Radiation Effects and Defects in Solids* 2012;167(1): 49-58.
- [46] KK Kumar, M Ravi, Y Pavani, S Bhavani, AK Sharma, VVRN Ro. *Phys B* 2011;406(9): 1706.
- [47] RG Linford. "Electrochemical Science and Technology of Polymers." Elsevier Appl. Sci., London, (1987), Chapter 3.
- [48] S Ramesh, KY Ng. *Current Appl Phys* 2009; 9(2): 329.